Mechanism of Inhibition of Human KSP by Monastrol: Insights from Kinetic Analysis and the Effect of Ionic Strength on KSP Inhibition†

Lusong Luo,*,‡ Jeffrey D. Carson,‡ Dashyant Dhanak,§ Jeffrey R. Jackson,|| Pearl S. Huang,|| Yan Lee,⊥ Roman Sakowicz,⊥ and Robert A. Copeland*,‡

Department of Enzymology and Mechanistic Pharmacology, MMPD CEDD, Department of Medicinal Chemistry, MMPD CEDD, and Department of Oncology, MMPD CEDD, GlaxoSmithKline, Collegeville, Pennsylvania 19426, and Cytokinetics Inc., 280 East Grand Avenue, South San Francisco, California 94080

Received August 10, 2004; Revised Manuscript Received September 20, 2004

ABSTRACT: Kinesin motor proteins utilize the energy from ATP hydrolysis to transport cellular cargo along microtubules. Kinesins that play essential roles in the mechanics of mitosis are attractive targets for novel antimitotic cancer therapies. Monastrol, a cell-permeable inhibitor that specifically inhibits the kinesin Eg5, the *Xenopus laevis* homologue of human KSP, can cause mitotic arrest and monopolar spindle formation. In this study, we show that the extent of monastrol inhibition of KSP microtubule-stimulated ATP hydrolysis is highly dependent upon ionic strength. Detailed kinetic analysis of KSP inhibition by monastrol in the presence and absence of microtubules suggests that monastrol binds to the KSP−ADP complex, forming a KSP−ADP−monastrol ternary complex, which cannot bind to microtubules productively and cannot undergo further ATP-driven conformational changes.

Mitotic kinesins play critical roles during discrete phases of mitosis (*3*−*5*). One such kinesin, KSP/*Hs*Eg5, in particular, is indispensable for bipolar spindle formation during mitosis (*3*−*5*). Inhibition of mitotic spindle assembly by disruption of microtubule dynamics has proven to be a successful means for treating cancer, exemplified by the clinical activity of the taxanes paclitaxel and docetaxel, and vinca alkaloids, vinblastine, vincristine, and vinorelbine. Inhibition of mitotic kinesins represents a promising alternative strategy for antiproliferative therapy (*6*−*9*). Monastrol, a cell-permeable inhibitor of Eg5, the *Xenopus laevis* homologue of the human kinesin KSP, was first reported by Mayer et al. (*10*) as an antimitotic agent that can cause mitotic arrest with monopolar spindles. The mechanism by which monastrol inhibits Eg5 function was later revealed by biochemical and structural studies (*11*−*13*). In two recent publications, Maliga et al. and DeBonis et al. (*11*, *12*) both showed that monastrol does not directly compete for ATP and microtubule (MT)[1] binding, suggesting that monastrol inhibits the ATPase activity of Eg5 by binding to an allosteric site. Earlier this year, the monastrol-bound KSP motor domain crystal structure was described by Yan et al. (*13*). The 1.9 Å resolution structure confirmed that monastrol is indeed an allosteric inhibitor that binds to an induced-fit pocket 12 Å away from the nucleotide binding pocket of KSP. The binding of monastrol triggers the downward swing of the insertion loop (loop L5) between helix α2 and helix α3 which generates a binding pocket. In addition to the conformational changes at the induced-fit site, structural changes also occur in the switch I and switch II regions of the protein.

In this study, we have investigated in detail the mechanism of inhibition of KSP by monastrol in the presence and absence of MTs by utilizing steady-state and transient-state kinetic techniques. We observed that the binding of monastrol to the KSP−MT complex is very sensitive to ionic strength. The kinetic analysis and the ionic strength-dependent inhibition of the KSP−MT complex by monastrol showed that monastrol preferentially binds to the KSP−ADP complex and locks this complex into a conformation not amendable for productive MT binding.

EXPERIMENTAL PROCEDURES

Materials. Monastrol was purchased from A. G. Scientific. Pyruvate kinase−lactate dehydrogenase enzymes, purine nucleoside phosphorylase, xanthine oxidase, and horseradish peroxidase were purchased from Sigma. The motor domain of KSP (amino acids 1−360) was expressed in *Escherichia coli* BL21(DE3) as a C-terminal six-His fusion protein (KSP360H). Bacterial pellets were lysed with a microfluidizer (Microfluidics Corp.) in lysis buffer [50 mM Tris-HCl, 50 mM KCl, 10 mM imidazole, 2 mM $MgCl_2$, 8 mM β-mercaptoethanol, and 0.1 mM ATP (pH 7.4)], and proteins were purified using Ni−NTA agarose affinity chromatography, with an elution buffer consisting of 50 mM PIPES, 10% sucrose, 300 mM imidazole, 50 mM KCl, 2 mM $MgCl_2$,

† Dedicated to Prof. Christopher T. Walsh on the occasion of his 60th birthday.

* To whom correspondence should be addressed. E-mail: lusong.luo@gsk.com or robert.a.copeland@gsk.com. Phone: (610) 917-7449. Fax: (610) 917-7901.

‡ Department of Enzymology and Mechanistic Pharmacology, MMPD CEDD, GlaxoSmithKline.-

§ Department of Medicinal Chemistry, MMPD CEDD, GlaxoSmithKline.

|| Department of Oncology, MMPD CEDD, GlaxoSmithKline.

⊥ Cytokinetics Inc.

[1] Abbreviations: AMP-PNP, adenosine 5′-(β,γ-imido)triphosphate; KSP, kinesin spindle protein; MT, microtubule; EGTA, ethylene glycol *O*,*O*′-bis(2-aminoethyl)-*N*,*N*,*N*′,*N*′-tetraacetic acid; ncd kinesin, non-Claret disjunctional kinesin; NTP, nucleotide 5′-triphosphate; NDP, nucleotide 5′-diphosphate.

10.1021/bi048282t CCC: $27.50
Published on Web 11/10/2004

1 mM β-mercaptoethanol, and 0.1 mM ATP (pH 6.8) as described in ref *8*.

Steady-State Kinetic Analysis of Human KSP ATPase Activity and Inhibition by Monastrol. Steady-state analyses were carried out using a pyruvate kinase−lactate dehydrogenase detection system that coupled the production of ADP to oxidation of NADH. Absorbance changes were monitored at 340 nm. For studies in which ADP was used as an inhibitor, a fluorescent phosphate detection assay was utilized. This assay detects free phosphate in solution through the formation of the fluorescent product resorufin by a purine nucleoside phosphorylase−xanthine oxidase−horseradish peroxidase coupling system. All biochemical experiments were performed in PEM25 buffer [25 mM PipesK$^+$ (pH 6.8), 2 mM $MgCl_2$, and 1 mM EGTA] supplemented with 10 μM paclitaxel for experiments involving microtubules and 0−150 mM KCl for ionic strength dependence studies. The IC_{50} for steady-state inhibition was determined at 500 μM ATP, 5 μM MTs, and 20 nM KSP, with different NaCl or KCl concentrations in PEM25 buffer. IC_{50} values were determined by fitting inhibition data to the binding isotherm (eq 1)

$$\frac{v}{v_0} = \frac{1}{1 + \left(\frac{[I]}{IC_{50}}\right)^n} \quad (1)$$

where v is the reaction velocity at different concentrations of inhibitor I, v_o is the control velocity in the absence of inhibitor, and n is the number of the inhibitor molecules bound to the enzyme.

Inhibitor modality under steady-state conditions was determined by measuring the effect of inhibitor concentration on initial velocity as a function of substrate concentration. For AMP-PNP and ADP inhibition of the KSP motor domain (30 nM) in the presence of MT, saturating MT (200 μg/mL) was used in the assay. The ADP concentrations used in the assay were 300, 100, 33, and 0 μM. The AMP-PNP concentrations used in the assay were 40, 13, 4.3, and 0 μM. The ATP concentrations were varied from 200 to 1.6 μM through a 2-fold serial dilution. Data were fit globally, using GraFit, to velocity equations for competitive, noncompetitive, uncompetitive, and mixed inhibition.

Mutual Exclusivity Studies. Mutual exclusivity studies were carried out by measuring the enzyme velocity while varying the monastrol concentration (2-fold serial dilution starting from 40 μM) at a series of fixed concentrations of AMP-PNP (400, 200, 100, 50, and 0 μM) or ADP (400, 200, 100, 50, and 0 μM) in the presence of a fixed MT concentration (100 μg/mL). The ATP concentration of the reaction solution was 100 μM. The experiment was performed in PEM25 buffer [25 mM PipesK$^+$ (pH 6.8), 2 mM $MgCl_2$, and 1 mM EGTA]. Data were fit globally to the equation of Yonetani and Theorell (eq 2) (*14*) by using GraFit:

$$\frac{1}{v_{ij}} = \frac{1}{v_0}\left(1 + \frac{[I]}{K_i} + \frac{[J]}{K_j} + \frac{[I][J]}{\alpha K_i K_j}\right) \quad (2)$$

where v_o is the velocity when no inhibitor is present, K_i and K_j are the apparent dissociation constants for inhibitors I and J, respectively, and α is a constant that defines the degree of interaction between the two inhibitors.

Determination of Monastrol Binding Constants by Fluorescence Titration. KSP tryptophan fluorescence titration experiments were carried out using a PTI fluorescence instrument. The excitation wavelength was 280 nm, and the emission spectra were recorded in the range of 310−420 nm for 3 mL solutions containing 0.1 μM KSP titrated with 0−12 μM monastrol. The observed fluorescence at 340 nm was plotted as a function of the monastrol concentration and the curve analyzed with eq 3 using GraFit (Erithacus Software).

$$\Delta F_{obs} = \Delta F_{max}/(1 + K_d/[L]) \quad (3)$$

ΔF_{obs} is the observed change in fluorescence, ΔF_{max} is the total change in fluorescence at a saturating concentration of L, K_d is the apparent dissociation constant of the ligand, and [L] is the concentration of monastrol.

Stopped-Flow Experiments. The rates of monastrol binding to KSP were determined by monitoring the fluorescence signal quenching of Trp127 within the loop 5 region (*15*). The excitation wavelength was 295 nm, and the emission filter cutoff was 320 nm. The stock solutions of monastrol (10−60 μM) and KSP360H (1 μM) in the presence of 500 μM ADP or 500 μM AMP-PNP in PEM25 buffer [25 mM PipesK$^+$ (pH 6.8), 2 mM $MgCl_2$, and 1 mM EGTA] were mixed with a stopped-flow apparatus (Hi-Tech Scientific). Data were collected in triplicate and then averaged. The fluorescence quenching traces were analyzed with a single-exponential equation to obtain the observed rate constants k_{obs} for KSP−ADP titrations and a double-exponential equation for the KSP−AMP-PNP titration. The plot of k_{obs} (or for the KSP−AMP-PNP titration, the k_{obs} for the fast phase) as a function of monastrol concentration was linear. These data were fit to eq 4 to obtain k_{on} and k_{off}.

$$k_{obs} = k_{off} + k_{on}[S] \quad (4)$$

where k_{on} and k_{off} are the association rate and dissociation rate constants, respectively, [S] is the ligand concentration, and k_{obs} is the observed rate constant.

RESULTS

Effect of Ionic Strength on the MT $K_{1/2}$ for KSP-Catalyzed ATP Hydrolysis. In the steady-state kinetic analyses, we determined the kinetic parameters for KSP motor domain-catalyzed ATP hydrolysis at different KCl concentrations. The construct we used for these studies is the truncated KSP motor domain, KSP360H (*8*), encoding the initial 360 amino acids of the core KSP motor domain and a portion of the neck linker with a carboxy-terminal hexahistidine tag. In the absence of MT, the basal KSP−ATP hydrolysis rate had a k_{cat} value of 0.10 ± 0.01 s^{-1} and the K_m for ATP was 2.0 ± 0.2 μM. Both basal KSP ATPase reaction constants k_{cat} and $K_{m,ATP}$ were not affected by the change in salt concentration (data not shown). In the presence of MT, the KSP360H ATPase activity was enhanced 140-fold to 14 s^{-1}, agreeing with previous reports (Table 1) (*11*, *12*). For the MT-stimulated ATP hydrolysis reaction catalyzed by KSP, neither the value of k_{cat} nor the $K_{m,ATP}$ was affected by the addition of KCl up to 150 mM (Table 1). This is in contrast to the previous characterizations of the ionic strength effects on the ATP hydrolysis by KSP (*11*) and its homologue *Xenopus* Eg5 (*2*), for which a drop in the maximum ATPase rate was

Table 1: Kinetic Parameters for Human KSP360H-Catalyzed ATP Hydrolysis

[KCl] (mM)	k_{cat} (s^{-1})	$K_{m,ATP}$ (μM)	$K_{1/2,MT}$ (μM)	$k_{cat}/K_{1/2,MT}$ (μM^{-1} s^{-1})
0	14 ± 1	15 ± 2	0.27 ± 0.01	52
50	14 ± 1	16 ± 1	0.48 ± 0.05	29
100	12 ± 1	13 ± 3	1.4 ± 0.1	9
150	18 ± 5	ND[a]	6 ± 1	3

[a] Not determined.

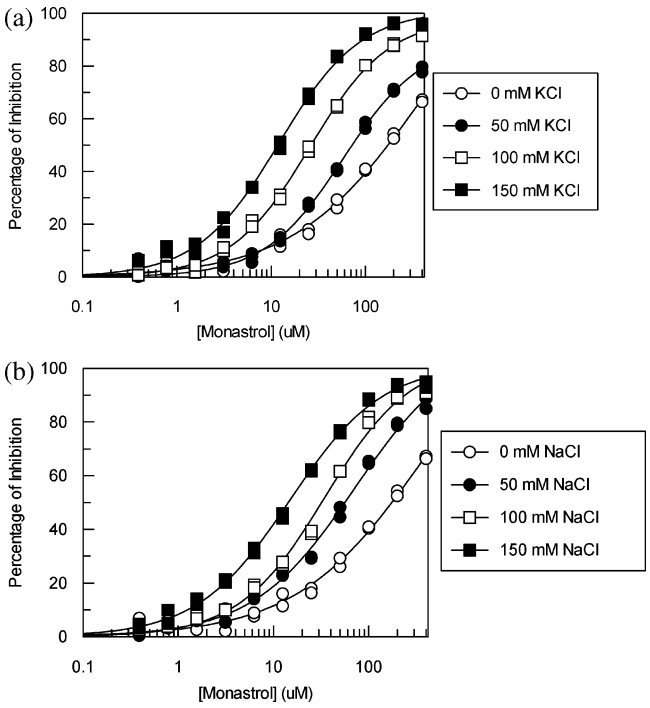

FIGURE 1: Inhibition of the MT-stimulated KSP360H ATPase activity by monastrol in the presence of (a) no additional KCl (○), 50 mM KCl (●), 100 mM KCl (□), and 150 mM KCl (■) or (b) no additional NaCl (○), 50 mM NaCl (●), 100 mM NaCl (□), and 150 mM NaCl (■). All reaction mixtures contained 20 nM KSP, 500 μM ATP, 5 μM MT, and PEM25 buffer [25 mM $PipesK^+$ (pH 6.8), 2 mM $MgCl_2$, and 1 mM EGTA].

reported. The $K_{1/2,MT}$ in the MT-stimulated KSP ATP hydrolysis, on the other hand, was very sensitive to ionic strength. The addition of 50, 100, and 150 mM KCl increased the $K_{1/2,MT}$ from 0.27 μM (at 0 mM KCl) to 0.48, 1.6, and 6 μM, respectively. Consequently, the $k_{cat}/K_{1/2,MT}$ values dropped 2-, 6-, and 17-fold, respectively. These results indicate that with the increase in KCl concentration, at any fixed nonsaturating concentration of MT, less MT is able to productively bind to the KSP motor domain to stimulate ATP hydrolysis. Therefore, the MT-stimulated KSP ATPase activity can be modulated by ionic strength by altering the strength of interactions (most likely electrostatic) between MT and the KSP motor domain.

Effect of Ionic Strength on Monastrol Inhibition of MT-Stimulated KSP ATP Hydrolysis. To examine the effect of ionic strength on the binding of monastrol to KSP, we carried out concentration−response studies of monastrol inhibition of KSP at different KCl concentrations. The IC_{50} values (median inhibitory concentration) were determined by measuring ATPase activity of KSP360H (20 nM) at 5 μM MT and 500 μM ATP with different KCl concentrations. Interestingly, the IC_{50} values shift with the increase in KCl

Table 2: Inhibition of Human KSP360H by Monastrol under Different Salt Concentrations (all IC_{50} values in units of micromolar)[a]

salt	IC_{50} (0 mM salt)	IC_{50} (50 mM salt)	IC_{50} (100 mM salt)	IC_{50} (150 mM salt)
KCl	~150	58 ± 4	25 ± 1	12 ± 1
NaCl	~150	71 ± 11	34 ± 3	15 ± 1

[a] The assay solution included 20 nM KSP, 500 μM ATP, 5 μM MTs, and PEM25 buffer [25 mM $PipesK^+$ (pH 6.8), 2 mM $MgCl_2$, and 1 mM EGTA].

concentration (Figure 1a). Similar results were obtained when NaCl was substituted for KCl (Figure 1b). Under these assay conditions where no additional salt was added (0 mM salt), the IC_{50} of monastrol for MT-stimulated KSP ATPase activity was estimated to be 150 μM (an accurate IC_{50} value under this condition could not be obtained due to the poor solubility of monastrol at concentrations above 400 μM). The presence of 50, 100, or 150 mM salt decreases the IC_{50} ~3-, ~6-, and ~10-fold, respectively (Table 2). This salt concentration-dependent IC_{50} shift suggests that the affinity of monastrol for KSP increases with an increase in ionic strength.

Mode of Inhibition of KSP by Monastrol. To understand the ionic strength dependence of KSP inhibition by monastrol, we studied the mode of inhibition of monastrol by steady-state kinetic analysis. The rates of basal KSP ATP hydrolysis in the presence of varying concentrations of ATP and monastrol were measured, and the data were fit globally using Grafit (Figure 2a). The Lineweaver−Burk plot clearly shows that monastrol is an ATP uncompetitive inhibitor in the basal KSP reaction with an inhibition constant (K_i) of 5.0 ± 0.2 μM. In the presence of MT, the steady-state mode of inhibition study showed that monastrol is again uncompetitive with respect to ATP (Figure 2b). These results show that monastrol does not compete for ATP binding, agreeing with the previous reports. Interestingly, the uncompetitive modality versus ATP in the presence or absence of MT suggests that monastrol has a higher affinity for nucleotide-bound forms of KSP than for nucleotide-free KSP.

The mode of inhibition studies with varying concentrations of MT and monastrol in the presence of a saturating concentration of ATP reveal that monastrol acts via a mixed (competitive-like) mechanism with respect to MT (Figure 2c) with a K_i of 5.6 ± 0.4 μM and a K_i' of 170 ± 40 μM. In this case, K_i is the inhibition constant of monastrol for KSP and K_i' is the inhibition constant of monastrol for the KSP−MT complex. The ca. 30-fold difference between K_i and K_i' suggests that monastrol binds much tighter to the form of KSP that cannot be productively bound and stimulated by MT. This result could explain the observed ionic strength dependence in monastrol inhibition of MT-stimulated KSP ATPase activity. As the strength of MT binding to the KSP motor domain is ionic strength-dependent, the increase in salt concentration will decrease the population of the KSP−MT complex and increase that of the free KSP species. As a result, the monastrol shows more inhibition under conditions where the salt concentration is higher. This hypothesis is supported by theoretical IC_{50} calculations using the Cheng and Prusoff relationship for noncompetitive (mixed-type) inhibition (eq 5) (*16*). The $K_{1/2,MT}$ under the different salt concentrations, monastrol K_i and α value determined in the steady-state kinetic analyses, and the MT

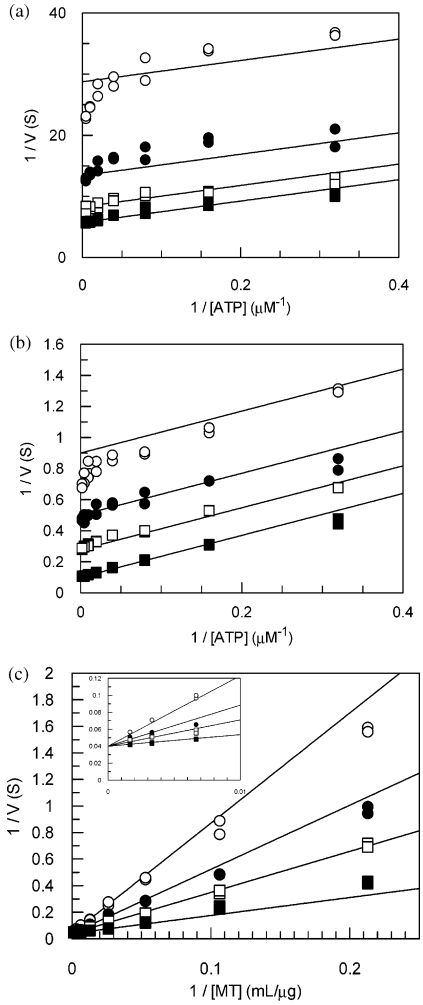

FIGURE 2: Studies of the mode of inhibition of monastrol by varying (a) the ATP concentration in the absence of MTs with 24 μM monastrol (○), 12 μM monastrol (●), 6 μM monastrol (□), and 0 μM monastrol (■), (b) the ATP concentration in the presence of a saturating MT concentration with 24 μM monastrol (○), 12 μM monastrol (●), 6 μM monastrol (□), and 0 μM monastrol (■), and (c) the MT concentration in the presence of a saturating ATP concentration with 24 μM monastrol (○), 12 μM monastrol (●), 6 μM monastrol (□), and 0 μM monastrol (■). The bottom left corner of panel c was expanded and displayed as an inset. The KSP360H concentration in these reactions was 500 nM for panel a and 30 nM for panels b and c. The Lineweaver−Burk plots were employed to show different modes of inhibition.

concentration used in the assay were used for theoretical IC_{50} calculations. As shown in Figure 3, the theoretical IC_{50} values calculated at different KCl concentrations correlate very well with the experimental values, confirming that the IC_{50} shifts indeed result from the different distribution of free KSP and the KSP−MT complex population at different ionic strengths.

$$IC_{50} = \frac{[S] + K_{1/2}}{\frac{K_{1/2}}{K_i} + \frac{[S]}{\alpha K_i}} \quad (5)$$

To further investigate whether the change in ionic strength has effects other than redistributing the free KSP and KSP−MT complex populations, we carried out mode of inhibition studies at different salt concentrations. Comparisons of K_i and K_i' values determined at 0, 50, and 100 mM KCl (with varied MT and monastrol concentrations and a saturating

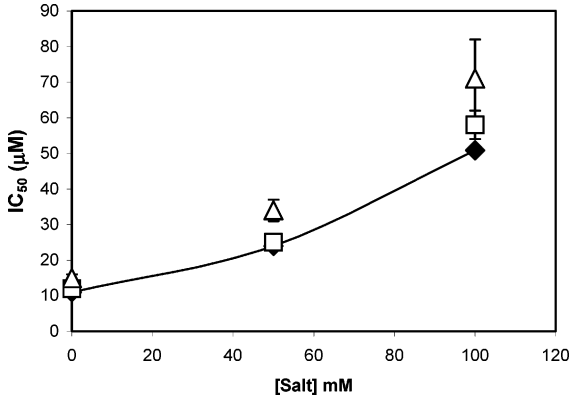

FIGURE 3: IC_{50} values determined from inhibition studies with varied KCl (□) and NaCl (△) concentrations. The IC_{50} values were fit by Cheng and Prusoff relationships (eq 5), and the theoretical IC_{50} values at salt concentrations of 0, 50, and 100 mM are also shown (◆).

Table 3: Monastrol Inhibition Constants for Human KSP Determined by Varying MT Concentrations at Different Salt Concentrations (20 nM KSP and 400 μM ATP)

[KCl] (mM)	K_i (μM)	K_i' (μM)	K_i'/K_i
0	5.6 ± 0.4	170 ± 40	30
50	4.4 ± 0.8	139 ± 60	31
100	5.0 ± 0.7	157 ± 50	31

Table 4: Inhibition Constants of AMP-PNP and ADP for the KSP Motor Domain in the Presence and Absence of Microtubules Determined by Fluorescent Phosphate Assay and PK/LDH Assay (see Experimental Procedures for details)

inhibitor	KSP K_i (μM)	KSP−microtubule K_i (μM)
AMP-PNP	98 ± 35[a] (92 ± 26[b])	13 ± 2[a] (7.0 ± 0.5[b])
ADP	1.5 ± 0.1[a]	92 ± 14[a]

[a] Fluorescent phosphate assay. [b] PK/LDH assay.

ATP concentration) show that the intrinsic affinity of monastrol for free KSP and the intrinsic affinity of monastrol for the KSP−MT complex are not affected by the ionic strength. These results verify that the change in ionic strength has no effect on the intrinsic binding affinity of monastrol for free KSP or the KSP−MT complex.

Mutual Exclusivity Studies. The catalytic core of the kinesin motors is significantly similar to myosins and small GTPases in the nucleotide-state-sensing machinery. All these classes of proteins are able to detect and differentiate between bound NTP and NDP and respond with conformational changes that alter the enzyme affinity for its protein binding partners, in the case of kinesin, the affinity for MTs (*17*−*21*). To determine the nucleotide binding conformation for which monastrol has the greatest affinity, we carried out mutual exclusivity studies of monastrol with ADP and with the ATP analogue AMP-PNP. The inhibition constants of ADP and AMP-PNP for the KSP motor domain in the presence and absence of microtubules were first tested. Both ADP and AMP-PNP exhibited competitive inhibition of ATP hydrolysis by the KSP motor domain in the presence or absence of MTs (Table 4). Without MTs, AMP-PNP binds to the KSP motor domain with a K_i of 98 ± 35 μM; the binding affinity increases more than 7-fold to 13 ± 2 μM when MTs are present. In contrast, ADP binds to the free KSP motor domain with a K_i of 1.5 ± 0.1 μM, and its binding affinity decreases ca. 60-fold to 92 ± 14 μM when

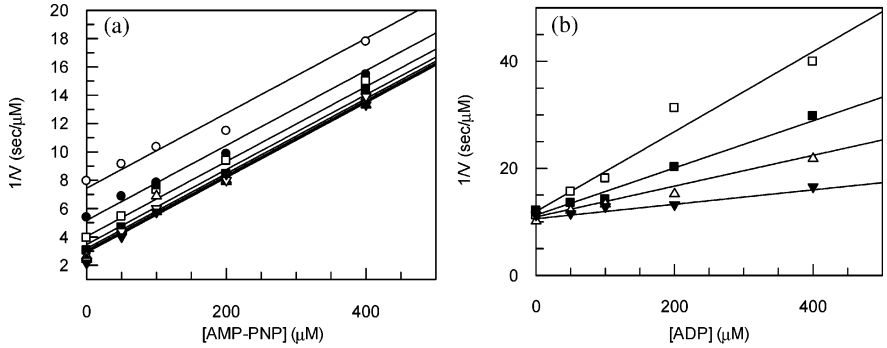

FIGURE 4: Yonetani−Theorell plots of the inhibition of the KSP ATPase (30 nM KSP) activity by monastrol in the presence of (a) AMP-PNP and (b) ADP (see Experimental Procedures for details).

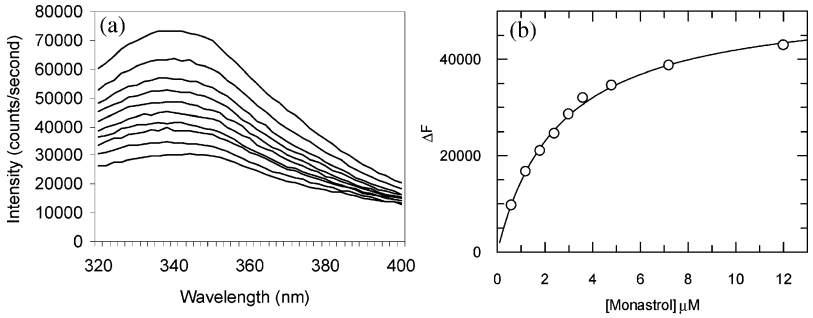

FIGURE 5: (a) Fluorescence emission spectra of 100 nM KSP360H (in PEM25 buffer at 25 °C) in the presence of 0−12 mM monastrol (from top to bottom). (b) Observed fluorescence change at 340 nm as a function of monastrol concentration. The curve was fitted by eq 3.

a saturating MT concentration is present in the assay solution. These results show that the presence of MT has a remarkable effect on the binding of ADP and AMP-PNP (ATP) to the KSP motor domain, in agreement with the previously presented hypothesis that there are two different nucleotide binding conformations associated with the binding and dissociation of MTs (*17*, *19*). In mutual exclusivity studies, measurements of the initial velocity of the enzymatic reaction at different combinations of monastrol and ADP or AMP-PNP were fit globally to the Yonetani−Theorell equation using Grafit. The term α in the Yonetani−Theorell equation is a constant that defines the degree of interaction between the two inhibitors. If the two inhibitors bind to the enzyme in a mutually exclusive manner, the value of α is infinite. When the two inhibitors are not mutually exclusive, $\alpha \neq \infty$. An α of <1 is indicative of positive cooperativity in the binding of the two inhibitors, and an α between 1 and ∞ signals antagonism in the binding of the two inhibitors (*22*). As shown in Figure 4, the global fittings for monastrol and AMP-PNP in the Yonetani−Theorell plots display parallel lines, indicating that monastrol and AMP-PNP bind to KSP in a mutually exclusive fashion in the presence of MTs. The combination of monastrol and ADP, on the other hand, yields lines that intersect above the *x*-axis. Calculation using eq 2 yields an α value of 0.03, which is an indication of strong binding synergy between monastrol and ADP. These results suggest that monastrol binds to KSP synergistically with ADP, but mutually exclusively with AMP-PNP. When two inhibitors are found to bind mutually exclusively with each other through kinetic analysis, there are two potential explanations: (1) the two inhibitors bind to a common site on the enzyme, or (2) the two inhibitors bind at independent sites that strongly affect each other through conformational communication (i.e., allostery) so that the occupation of one site precludes ligand binding at the second site. In this case, it is known from a combination of kinetic and structural studies that monastrol does not bind to the nucleotide binding site (*11*−*13*). Hence, it is most likely that monastrol and AMP-PNP bind to two different conformations of KSP; binding of one ligand will likely lock the enzyme out of the alternative conformation. The strong synergism observed between monastrol and ADP further supports this hypothesis.

Determination of Equilibrium Binding Constants for Monastrol−KSP Motor Domain Binding by Fluorescence Titration. The crystal structure of KSP in complex with monastrol and Mg^{2+}·ADP shows that monastrol binds to an induced-fit pocket, situated between helix α3 and loop L5 of helix α2 (*13*). Once monastrol binds, loop L5 moves downward ∼7 Å and the side chain of Trp127, which is located at the tip of loop L5, moves ∼10 Å to cap the entrance of the newly formed pocket. Since Trp127 is the only tryptophan residue in the KSP360H motor domain construct, the fluorescence signal from Trp127 can be used as a probe to detect the binding of monastrol to KSP (*15*). In the equilibrium fluorescence titration experiment, we observed the expected fluorescence quenching upon titration of monastrol to the KSP solution. In this experiment, aliquots of monastrol were added to a 100 nM KSP solution. The solution was mixed after each aliquot was added, and the fluorescence intensity was recorded as the average of a 1 min reading. The fluorescence titration spectra of 100 nM KSP measured in the presence of 0−12 μM monastrol are shown in Figure 5a, and the titration curve determined at 340 nm and fit by eq 3 is shown in Figure 5b. The K_d value obtained by the fitting is 2.6 ± 0.1 μM, in good agreement with the inhibition constant (5.0 μM) determined for the basal KSP inhibition and 5.4 μM (K_i) for inhibition of KSP with a saturating MT concentration. To test whether the observed signal quenching was directly correlated with monastrol binding, we used ADP as a control, which is known to bind

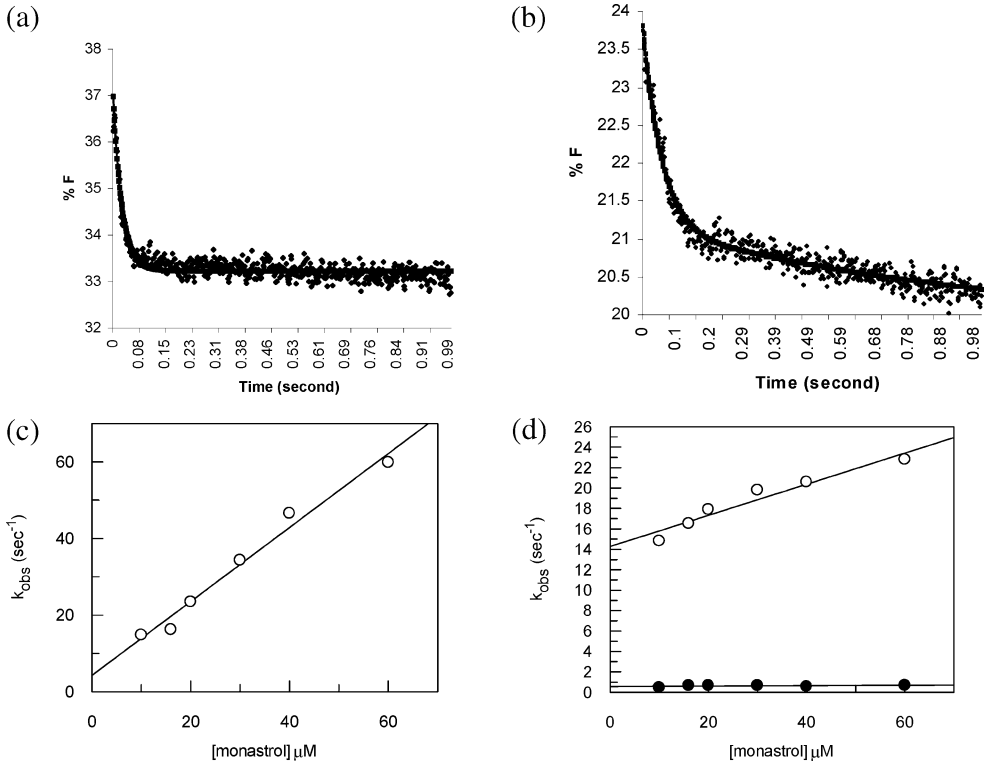

FIGURE 6: (a) Binding transients obtained after mixing 1 μM KSP360H and 40 μM monastrol in the presence of 500 μM ADP. The scattered dots represent an average of three repeated experiments collected by the stopped-flow apparatus, and the solid lines represent the best fit to the data. (b) Binding transients obtained after mixing 1 μM KSP360H and 40 μM monastrol in the presence of 500 μM AMP-PNP. The scattered dots represent average values from three repeated experiments collected by the stopped-flow apparatus, and the solid lines represent the best fit to the data. (c) Pseudo-first-order rate constant (○, fitted by single-exponential equations) of monastrol binding to the KSP−ADP complex as a function of monastrol concentration. The data were fit to a linear equation. (d) Pseudo-first-order rate constants [fitted by a biexponential equation, the rates for the fast phase (○) and the rates for the slow phase (●) are presented] of binding of monastrol to the KSP−AMP-PNP complex as a function of monastrol concentration. The data were again fit to a linear equation.

tightly to the nucleotide binding site but not to interact with the loop L5 region. No fluorescence quenching was observed up to 60 μM ADP, confirming that the observed fluorescence quenching was indeed a result of specific binding of monastrol to the loop L5 region.

Determination of the Pre-Equilibrium Binding Rate for Binding of Monastrol to KSP. The fluorescence quenching of Trp127 was further utilized to determine the pre-equilibrium binding rate for binding of monastrol to KSP. The rate of monastrol binding to KSP was monitored in the stopped-flow apparatus after the rapid mixing of 1 μM KSP360H and various concentrations of monastrol (10−60 μM). The binding reactions were treated as pseudo-first-order since the monastrol concentrations were at least 10-fold larger than the enzyme concentration. Interestingly, the fluorescence decay curves were different for monastrol binding to KSP in the presence of ADP compared to its binding to KSP in the presence of AMP-PNP. As shown in panels a and b of Figure 6, the curves fit best to a single-exponential equation for monastrol binding to the KSP−ADP complex. In contrast, the presence of 500 μM AMP-PNP renders the binding event biphasic and the curves fit best to a biexponential equation for KSP−AMP-PNP binding. A close look at the fitting showed that only the fast phase was monastrol concentration-dependent for KSP−AMP-PNP binding (Figure 6d). The slow phase was not dependent on the monastrol concentration and was more than 1 order of magnitude slower than the fast phase. It is likely that the slow phase reflects the conformational change that the KSP−AMP-PNP complex undergoes upon monastrol binding. In a very recent publication, Wojcik et al. (*23*) studied the difference FT-IR spectra of Eg5−monastrol−ADP and Eg5−monastrol−ATP complexes. They observed notable conformational differences in the peptide backbone and differences in interactions of Eg5 with nucleotide phosphate moieties in those two complexes. It will be interesting to test whether the slow phase of monastrol binding to the KSP−AMP-PNP complex can be monitored by difference FT-IR and whether the nature of the conformational change can thus be better understood.

Table 5: Association Rate Constants (k_{on}) and Dissociation Rate Constants (k_{off}) Determined for Binding of Monastrol to KSP360H in the Presence of ADP or AMP-PNP

	k_{on} (μM^{-1} s^{-1})	k_{off} (s^{-1})
monastrol with KSP−ADP	0.97 ± 0.07	4.2 ± 2.3
monastrol with KSP−AMP-PNP	0.15 ± 0.02	14 ± 1

The k_{on} and k_{off} rates were determined by fitting the experimental data to eq 5 using the k_{obs} obtained from the single-exponential fitting for KSP−ADP binding and the fast phase k_{obs} derived from the two-exponential fitting for KSP−AMP-PNP binding. As shown in Table 5, the association rate constant for binding of monastrol to KSP360H in the presence of 500 μM ADP was determined to be 0.97 ± 0.07 μM^{-1} s^{-1} (closely matching the value of 0.8 μM^{-1} s^{-1} measured in ref *11*), while the k_{on} slowed more than 6-fold to 0.15 ± 0.01 μM^{-1} s^{-1} when ADP was replaced with AMP-PNP. On the other hand, the release of monastrol from the KSP−ADP complex was ~3-fold slower than its release

from the KSP−AMP-PNP complex. The binding constants calculated from the k_{on} and k_{off} values, determined from pre-equilibrium binding experiments, were 4.3 μM for binding of monastrol to the KSP−ADP complex and 93 μM for binding of monastrol to the KSP−AMP-PNP complex. These results suggest that monastrol has a higher affinity for the KSP−ADP complex than for the KSP−AMP-PNP complex, similar to the results obtained by the mutual exclusivity studies. In that case, with the MT present, monastrol exhibits better binding to KSP in the presence of ADP and no binding to the KSP−AMP-PNP complex.

DISCUSSION

Human KSP, also known as HsEg5, plays a crucial role in the establishment of spindle bipolarity (*24*, *25*). Malfunction of KSP leads to cell cycle arrest and monopolar spindle formation (*8*, *10*, *25*). The abundant expression of KSP in proliferating human tissues and the absence of KSP in postmitotic neurons (*8*) make it an attractive target for the discovery of novel and specific antimitotic cancer therapies. Monastrol has proven to be a useful tool with which to study KSP function during mitosis (*6*, *26*). In addition, the investigation of the mechanism of action of monastrol could provide new insights for the design of more potent KSP inhibitors. In this study, we carried out detailed kinetic analysis of monastrol inhibition of KSP ATPase activity in the presence and absence of MTs. The data presented in this study show that the monastrol inhibition of MT-stimulated KSP ATPase activity is very sensitive to ionic strength. It was previously known that salt concentration can affect the MT-stimulated kinesin ATPase activity (*2*, *27*−*30*). Lockhart and Cross (*2*) investigated the effect of ionic strength on MT-activated ATP hydrolysis by an Eg5(12−437GST) construct. They reported that the k_{cat} of the ATP hydrolysis reaction decreased more than 2-fold when the salt concentration was increased from 25 to 100 mM, while the $K_{1/2,MT}$ value decreased slightly. These observations are in sharp contrast with the significant increase in the $K_{1/2,MT}$ value we report. We also tested the KSP(12−437)[2] construct with a GST tag and observed an increase in $K_{1/2,MT}$ similar to that observed for KSP360 (data not shown). We have started investigating the detailed kinetic mechanism and the effect of salt concentration on monastrol inhibition of this dimeric construct. The dramatic increase in $K_{1/2,MT}$ and the very small change in k_{cat} suggested that the ionic strength affects the MT-activated KSP360 ATPase activity mainly through disrupting the interaction between MT and the kinesin motor domain. At higher salt concentrations, less MT can bind to KSP and thereby stimulate KSP ATPase activity. These results are consistent with the findings in studies of conventional kinesin and ncd (*31*, *32*).

In the mode of inhibition study, monastrol displayed mixed competitive-like inhibition with respect to MT with a K_i'/K_i ratio as large as 30; this large K_i'/K_i ratio suggests that monastrol binds to the KSP−MT complex 30-fold less effectively than to the MT-free state of KSP. Consequently, the inhibition of MT-stimulated KSP ATPase activity will be modulated by the ionic strength of the reaction solution as the distribution of KSP between MT-bound and MT-free states changes with the shift in ionic strength. Our calculation, based on Cheng and Prusoff relationships (*16*), shows that the ionic strength-dependent IC_{50} shifts could be predicted by the $K_{1/2,MT}$ data at different salt concentrations. The good agreement between experimental data and theoretical calculation further supports the model that the ionic strength dependence of monastrol inhibition of MT-stimulated KSP ATPase activity results from the ionic strength dependence of KSP−MT binding. It is worth noting that under physiological conditions the intracellular ionic strength is close to that of 150 mM KCl (*28*, *33*), significantly higher than the ionic strength of the typical KSP inhibition assay solution *in vitro* (*11*−*13*). Hence, the ionic strength factor should be taken into consideration when KSP inhibitors, such as monastrol, are evaluated. In the recent publication by DeBonis et al., the authors asked "why monastrol is so effective for mitotic cell arrest *in vivo* but not as effective *in vitro*" (*11*). We surmise that one of the reasons could be that the *in vitro* potency of monastrol was underestimated using biochemical assay conditions at low ionic strengths. As an allosteric inhibitor, monastrol does not directly compete for substrate binding, and hence does not have to compete with high cellular ATP concentrations or high local concentrations of microtubules in the mitotic spindles. However, since monastrol shows the highest affinity for the KSP−ADP complex and the population of the KSP domain as a KSP−ADP complex is affected by the local concentration of ATP and MTs, the KSP inhibition by monastrol is indeed sensitive to both ATP and MT concentrations.

Numerous biochemical and biophysical studies have suggested that kinesin motor domains assume two different nucleotide binding conformations: an ATP-bound conformation (or AMP-PNP-bound conformation) and an ADP-bound conformation (*17*−*20*). In this study, we showed that AMP-PNP and ADP have different affinities for the free KSP motor domain and the KSP−MT complex, with AMP-PNP binding favorably to the KSP−MT complex and ADP to free KSP. In the mutual exclusivity study, monastrol was shown to have strong binding synergy with ADP but binds mutually exclusively with AMP-PNP. Pre-equilibrium binding data further showed that monastrol binds to the KSP motor domain with a faster binding rate and slower dissociation rate in the presence of ADP than in the presence of AMP-PNP, confirming that it is the ADP form of the KSP motor domain that is the preferred binding partner for monastrol. In the steady-state mode of inhibition study, monastrol was shown to be uncompetitive with respect to ATP in the presence and absence of MTs, suggesting that monastrol's inhibitory effect can occur only after KSP binds to nucleotide. Taken together, these results suggest that monastrol binds to the KSP−ADP complex to lock KSP in a KSP−ADP−monastrol ternary complex that cannot go through the ATPase cycle (Figure 7). In contrast, the binding affinity of monastrol for the KSP−MT−ADP complex is much lower, forcing most of the monastrol to bind to the KSP−ADP complex. It is not yet clear whether the KSP−ADP−monastrol complex can bind to MTs (Figure 7). Crevel et al. recently proposed that monastrol stabilizes an attached low friction mode of KSP (*34*). They showed in their motility assays that the ternary Eg5−ADP−monastrol complex might be able to bind MTs in a low-friction fashion without

[2] We also tested a predicted dimer (*1*, *2*) KSP construct, KSP(12−437), with a GST tag and a comparable observed MT $K_{1/2}$ shift.

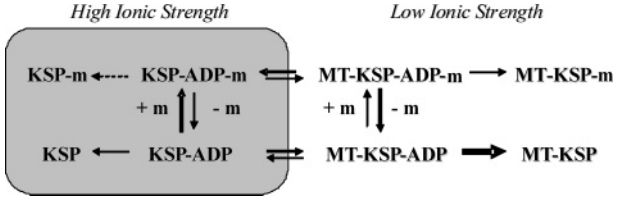

FIGURE 7: Proposed model explaining the effects of ionic strength on inhibition of the KSP ATPase reaction by monastrol (m).

productive ATP hydrolysis and coupled conformational changes. If this model is correct, it would be interesting to know how ionic strength affects this low-friction binding and whether this nonproductive KSP−ADP−monastrol−MT complex can be identified kinetically.

In summary, we report in this study detailed kinetic analysis of KSP inhibition by monastrol in the presence and absence of microtubules. These studies provide evidence that monastrol binds to the KSP−ADP complex much better than any other KSP binding complexes along the nucleotidase cycle. It is also observed that the inhibition of KSP microtubule-stimulated ATP hydrolysis by monastrol is very sensitive to ionic strength, resulting from the different distribution of free KSP and KSP−MT complex populations at different ionic strengths. These findings are important to the understanding of small-molecule inhibitors that target KSP and related kinesin motor proteins.

NOTE ADDED AFTER ASAP POSTING

This paper was inadvertently published 11/10/04. The salt concentrations associated with the IC_{50} values in Table 2 have been corrected to millimolar (mM), and the units of micromolar (μM) for the IC_{50} values have been added to the title of Table 2. The correct version of the paper was published 11/11/04.

ACKNOWLEDGMENT

Dr. Peter Tummino and Dr. Ken Wood are gratefully acknowledged for a careful reading of the manuscript.

REFERENCES

1. Funk, C. J., Davis, A. S., Hopkins, J. A., and Middleton, K. M. (2004) Development of high-throughput screens for discovery of kinesin adenosine triphosphatase modulators, *Anal. Biochem. 329*, 68−76.
2. Lockhart, A., and Cross, R. A. (1996) Kinetics and motility of the Eg5 microtubule motor, *Biochemistry 35*, 2365−2373.
3. Goldstein, L. S. (2001) Molecular motors: from one motor many tails to one motor many tales, *Trends Cell Biol. 11*, 477−482.
4. Mandelkow, E., and Mandelkow, E. M. (2002) Kinesin motors and disease, *Trends Cell Biol. 12*, 585−591.
5. Severson, A. F., and Bowerman, B. (2002) Cytokinesis: closing in on the central spindle, *Dev. Cell 2*, 4−6.
6. Miyamoto, D. T., Perlman, Z. E., Mitchison, T. J., and Shirasu-Hiza, M. (2003) Dynamics of the mitotic spindle: potential therapeutic targets, *Prog. Cell Cycle Res. 5*, 349−360.
7. Peterson, J. R., and Mitchison, T. J. (2002) Small molecules, big impact: a history of chemical inhibitors and the cytoskeleton, *Chem. Biol. 9*, 1275−1285.
8. Sakowicz, R., Finer, J. T., Beraud, C., Crompton, A., Lewis, E., Fritsch, A., Lee, Y., Mak, J., Moody, R., Turincio, R., Chabala, J. C., Gonzales, P., Roth, S., Weitman, S., and Wood, K. W. (2004) Antitumor activity of a kinesin inhibitor, *Cancer Res. 64*, 3276−3280.
9. Wood, K. W., Cornwell, W. D., and Jackson, J. R. (2001) Past and future of the mitotic spindle as an oncology target, *Curr. Opin. Pharmacol. 1*, 370−377.
10. Mayer, T. U., Kapoor, T. M., Haggarty, S. J., King, R. W., Schreiber, S. L., and Mitchison, T. J. (1999) Small molecule inhibitor of mitotic spindle bipolarity identified in a phenotype-based screen, *Science 286*, 971−974.
11. DeBonis, S., Simorre, J. P., Crevel, I., Lebeau, L., Skoufias, D. A., Blangy, A., Ebel, C., Gans, P., Cross, R., Hackney, D. D., Wade, R. H., and Kozielski, F. (2003) Interaction of the mitotic inhibitor monastrol with human kinesin Eg5, *Biochemistry 42*, 338−349.
12. Maliga, Z., Kapoor, T. M., and Mitchison, T. J. (2002) Evidence that monastrol is an allosteric inhibitor of the mitotic kinesin Eg5, *Chem. Biol. 9*, 989−996.
13. Yan, Y., Sardana, V., Xu, B., Homnick, C., Halczenko, W., Buser, C. A., Schaber, M., Hartman, G. D., Huber, H. E., and Kuo, L. C. (2004) Inhibition of a mitotic motor protein: where, how, and conformational consequences, *J. Mol. Biol. 335*, 547−554.
14. Yonetani, T., and Theorell, H. (1964) Studies on liver alcohol hydrogenase complexes. 3. Multiple inhibition kinetics in the presence of two competitive inhibitors, *Arch. Biochem. Biophys. 106*, 243−251.
15. Sakowicz, R. (2002) Methods for screening and therapeutic applications of kinesin modulators, U.S. Patent 10/427175-[US6440686].
16. Cheng, Y., and Prusoff, W. H. (1973) Relationship between the inhibition constant (K_I) and the concentration of inhibitor which causes 50% inhibition (I_{50}) of an enzymatic reaction, *Biochem. Pharmacol. 22*, 3099−3108.
17. Kikkawa, M., Sablin, E. P., Okada, Y., Yajima, H., Fletterick, R. J., and Hirokawa, N. (2001) Switch-based mechanism of kinesin motors, *Nature 411*, 439−445.
18. Kull, F. J., and Endow, S. A. (2002) Kinesin: switch I & II and the motor mechanism, *J. Cell Sci. 115*, 15−23.
19. Naber, N., Minehardt, T. J., Rice, S., Chen, X., Grammer, J., Matuska, M., Vale, R. D., Kollman, P. A., Car, R., Yount, R. G., Cooke, R., and Pate, E. (2003) Closing of the nucleotide pocket of kinesin-family motors upon binding to microtubules, *Science 300*, 798−801.
20. Sosa, H., Peterman, E. J., Moerner, W. E., and Goldstein, L. S. (2001) ADP-induced rocking of the kinesin motor domain revealed by single-molecule fluorescence polarization microscopy, *Nat. Struct. Biol. 8*, 540−544.
21. Yun, M., Zhang, X., Park, C. G., Park, H. W., and Endow, S. A. (2001) A structural pathway for activation of the kinesin motor ATPase, *EMBO J. 20*, 2611−2618.
22. Yonetani, T., and Theorell, H. (1964) Studies on liver alcohol hydrogenase complexes. 3. Multiple inhibition kinetics in the presence of two competitive inhibitors, *Arch. Biochem. Biophys. 106*, 243−251.
23. Wojcik, E. J., Dalrymple, N. A., Alford, S. R., Walker, R. A., and Kim, S. (2004) Disparity in allosteric interactions of monastrol with Eg5 in the presence of ADP and ATP: a difference FT-IR investigation, *Biochemistry 43*, 9939−9949.
24. Blangy, A., Lane, H. A., d'Herin, P., Harper, M., Kress, M., and Nigg, E. A. (1995) Phosphorylation by p34cdc2 regulates spindle association of human Eg5, a kinesin-related motor essential for bipolar spindle formation in vivo, *Cell 83*, 1159−1169.
25. Kapoor, T. M., Mayer, T. U., Coughlin, M. L., and Mitchison, T. J. (2000) Probing spindle assembly mechanisms with monastrol, a small molecule inhibitor of the mitotic kinesin, Eg5, *J. Cell Biol. 150*, 975−988.
26. Kapoor, T. M., and Mitchison, T. J. (2001) Eg5 is static in bipolar spindles relative to tubulin: evidence for a static spindle matrix, *J. Cell Biol. 154*, 1125−1133.
27. Gilbert, S. P., Webb, M. R., Brune, M., and Johnson, K. A. (1995) Pathway of processive ATP hydrolysis by kinesin, *Nature 373*, 671−676.
28. Hackney, D. D., and Stock, M. F. (2000) Kinesin's IAK tail domain inhibits initial microtubule-stimulated ADP release, *Nat. Cell Biol. 2*, 257−260.
29. Ma, Y. Z., and Taylor, E. W. (1997) Kinetic mechanism of a monomeric kinesin construct, *J. Biol. Chem. 272*, 717−723.
30. Stock, M. F., Chu, J., and Hackney, D. D. (2003) The kinesin family member BimC contains a second microtubule binding region attached to the N terminus of the motor domain, *J. Biol. Chem. 278*, 52315−52322.
31. Lockhart, A., and Cross, R. A. (1994) Origins of reversed directionality in the ncd molecular motor, *EMBO J. 13*, 751−757.

32. Ma, Y. Z., and Taylor, E. W. (1995) Mechanism of microtubule kinesin ATPase, *Biochemistry 34*, 13242−13251.
33. Heeley, D. H., and Smillie, L. B. (1988) Interaction of rabbit skeletal muscle troponin T and F-actin at physiological ionic strength, *Biochemistry 27*, 8227−8232.
34. Crevel, I. M., Alonso, M. C., and Cross, R. A. (2004) Monastrol stabilises an attached low-friction mode of Eg5, *Curr. Biol. 14*, R411−R412.

BI048282T